主办 中国科学院遥感与数字地球研究所
中国地理学会环境遥感分会
出版 科学出版社

JOURNAL OF REMOTE SENSING

遥感学报

2013年 Vol.17 第17卷 No.4 第4期 ISSN 1007-4619 CN11-3841 / TP CODEN YXAUAB

2010年中国土地覆被遥感监测数据集（ChinaCover2010）

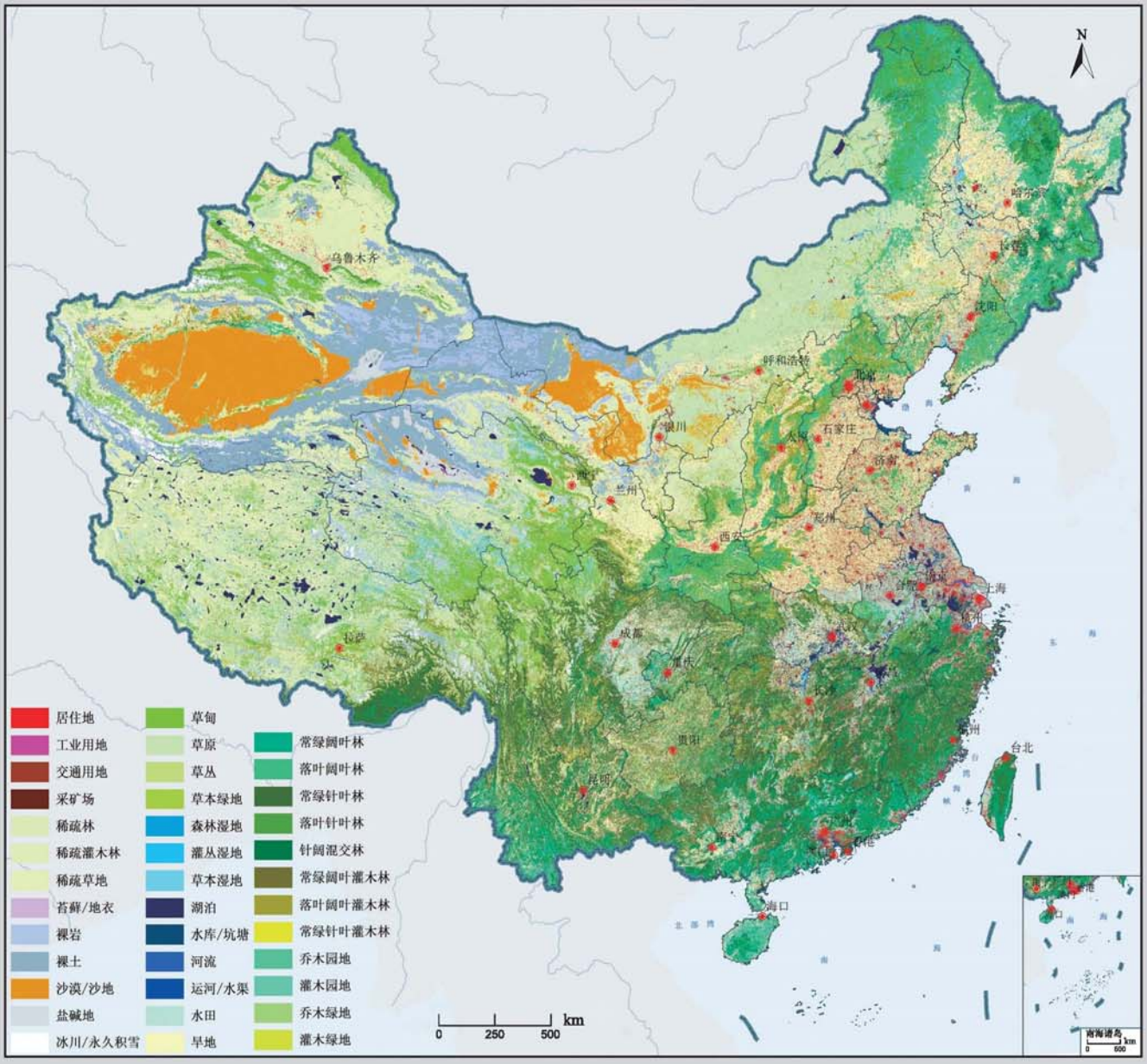

百种中国杰出学术期刊

遥感学报

Yaogan Xuebao

第 17 卷　　第 4 期　　2013 年 7 月

目　　次

JOURNAL OF REMOTE SENSING

(Vol. 17 No. 4 July, 2013)

CONTENTS

(to be continued to Inside Back Cover)

(continued from Contents page)

Haze: Remote Sensing

Joint use of active and passive remote sensing for monitoring of severe haze pollution in Beijing 2013

LI Zhengqiang, XU Hua, ZHANG Ying, ZHANG Yuhuan, CHEN Cheng, LI Donghui, LI Li, HOU Weizhen, LV Yang, GU Xingfa

State Environmental Protection Key Laboratory of Satellite Remote Sensing, Institute of Remote Sensing and Digital Earth, Chinese Academy of Sciences, Beijing 100101, *China*

Abstract: Focusing on the serious haze event in January 2013 in Beijing, we analyzed remote sensing results of haze aerosol properties based on passive-active joint monitoring approaches. The analyses show that the active remote sensing approaches have advantages during the high pollution cases or the nighttime, while the passive approaches provide more information for aerosol characterization. By joint use of ground-based site, vertical profile, and satellite coverage monitoring, one can preliminarily realize the stereoscopic observation of haze aerosols.

Key words: Haze, aerosol, remote sensing, ground-based LiDAR, active and passive remote sensing monitoring

CLC number: TP751 **Document code**: A

Citation format: **Li Z Q, Xu H, Zhang Y, Zhang Y H, Chen C, Li D H, Li L, Hou W Z, Lv Y and Gu X F. 2013. Joint use of active and passive remote sensing for monitoring of severe haze pollution in Beijing 2013. Journal of Remote Sensing, 17(4): 919-928 [DOI: 10.11834/jrs.20133066]**

1 INTRODUCTION

In January 2013, severe haze pollution occurred in most of China East region. It was counted for 5 times in Beijing for Air Quality Index (AQI) beyond 200 (severe pollution). In Fig.1, we show AQI monitoring results at Olympic center station provided by Beijing municipal environmental monitoring center. From AQI time series, the haze pollution process can be clearly identified from the figure which includes five severe pollution peaks occurred on January 6—8, 10—14, 18—19, 21—23 and 26—31. During these severe pollution cases, the primary pollutant was found to be Fine Particle Matters ($PM_{2.5}$). In the same figure, we show also the daily averaged $PM_{2.5}$ obtained at US embassy located at Chaoyang district of Beijing. The identical time variation of AQI and $PM_{2.5}$ proves that $PM_{2.5}$ is the dominant factor of this severe pollution event. From $PM_{2.5}$ figure, we identified five days with the maximum pollution level on January 7, 12, 18, 23 and 29. On January 12, the daily averaged $PM_{2.5}$ reached 552 $\mu g/m^3$ which was about 7 times larger than the limitation (75 $\mu g/m^3$) of The class environmental region of China (GB3095-2012). The number of polluted days (beyond the environmental pollution limitation) was 23 which counted 74% of the month, among which 16 days exceeded the severe pollution limitation counting 52% of the month. Such kind of severe atmospheric pollution can cause important health damage (Dockery, et al., 1993; Pope, et al., 2002) including angiocarpy and respiratory diseases and other environmental problems.

The formation of severe haze pollution in January 2013 in Beijing related closely to the static stability states of the atmosphere, and thus an analysis of metrological factors can help to understand the formation of the haze event. In Fig.2, we show the visibility, ambient humidity and wind speed obtained at Beijing southern metearological station. By comparison with Fig.1, we find that (1) there is clearly negative correlation between visibility and $PM_{2.5}$ which indicates significant influence of fine particle matters on the atmospheric visibility; (2) there is positive correlation between wind speed and dispersion of severe haze. With the increase of wind speed, the severe haze is removed and the visibility increases significantly. With the decrease of wind speed, haze accumulates in the atmosphere and visibility decreases continuously; (3) ambient humidity plays an important role in the formation of extreme haze pollution, e.g., on 12, 23 and 29 January. The hydroscopic increase of haze particle matters is exacerbated by the abundant water vapor when humidity higher than 80% which results in the quickly augmentation of the particle size.

2 REMOTE SENSING OBSERVATION AND ANALYSIS

By the joint use of active and passive remote sensing approaches, the stereoscopic monitoring of haze process can be

Received: 2013-03-26; **Accepted**: 2013-05-21; **Version of record first published**: 2013-05-28

Foundation: National Major Scientific Research Program (No.2010CB950800, 2010CB950801); Outstanding Youth Science Fund Project of National Natural Science Foundation of China (No.41222007)

First author biography: LI Zhengqiang (1977—), male, professor, his research interest is atmospheric remote sensing, E-mail: lizq@irsa.ac.cn

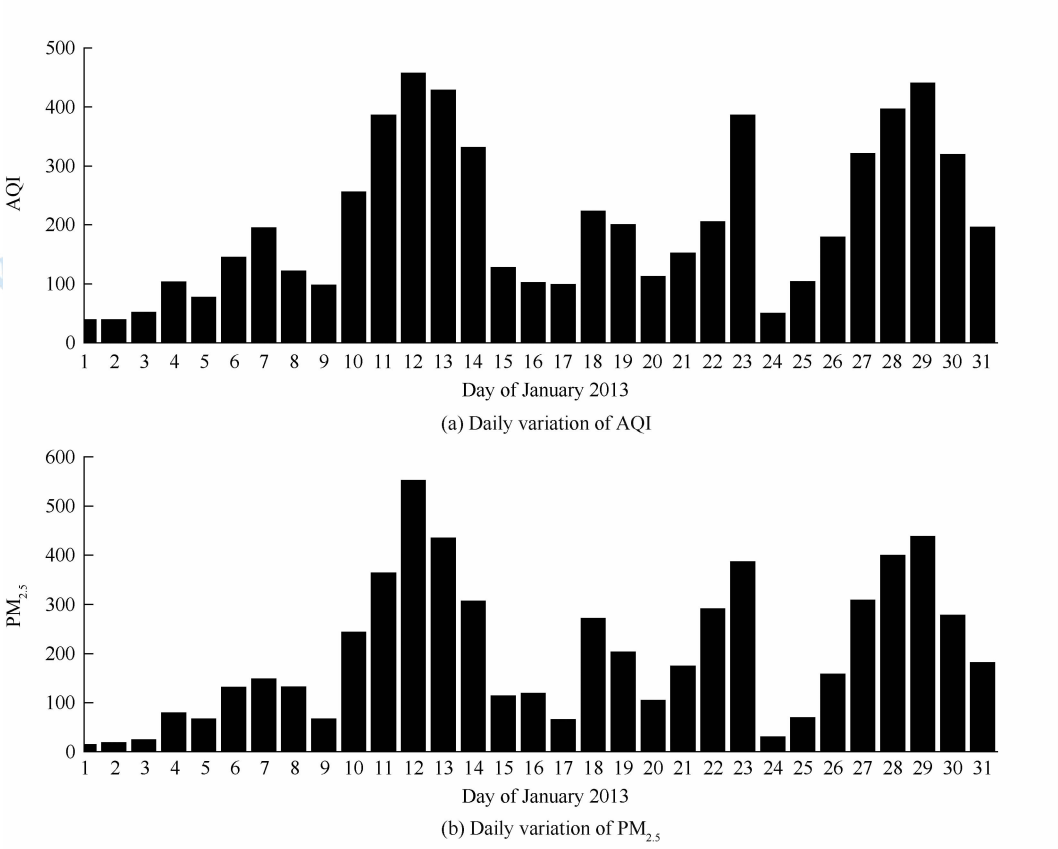

Fig.1 Daily averaged AQI and $PM_{2.5}$ contents ($\mu g/m^3$) in January 2013 at Beijing

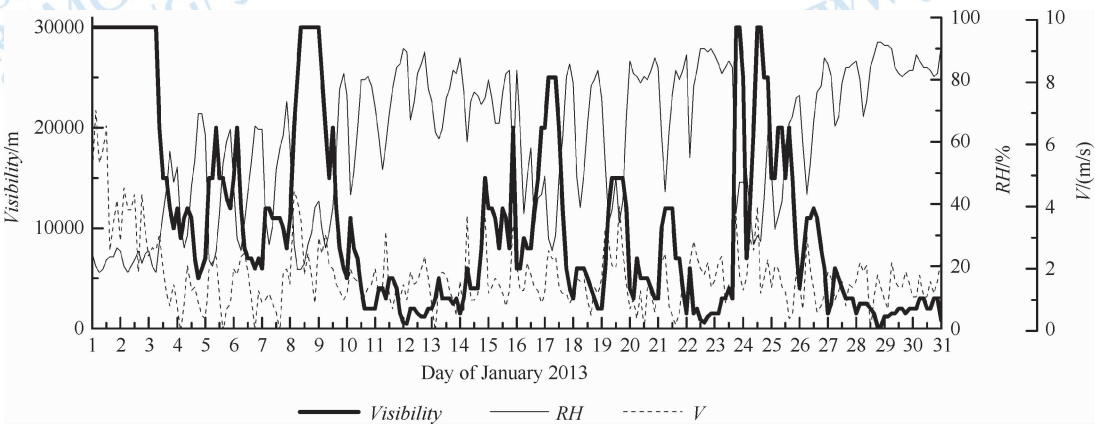

Fig.2 Atmospheric visibility, ambient humidity (*RH*) and wind speed (V) in January 2013 at Beijing

realized. In Fig.3, we show observation of the first haze pollution event of 2013 (January 5 to 8) based on ground-based LiDAR (CE370-2 manufactured by CIMEL, France, 532 nm, 150 mW with Nd:YAG laser) and sun-sky radiometer (CE318-DP manufactured by CIMEL, wavelength ranging from 340 nm to 1640 nm) at the observation site of Institute of Remote Sensing and Digital Earth (RADI), Chinese Academy of Sciences. In the same figure, we show also the hourly averaged $PM_{2.5}$ measured at US embassy located about 10 km away from RADI site. From Fig.3, we find that (1) in this haze pollution event, $PM_{2.5}$ shows a complete increase-to-decrease process. The atmospheric total column Aerosol Optical Depth (AOD) at 440 nm measured by sun-sky radiometer shows the maximum value of 1.19 which is about 10 times larger than the minimum value of 0.12. The coincident surface level $PM_{2.5}$ monitoring shows the similar multiple relationships; (2) LiDAR observation shows clearly the vertical distribution and variation of the atmospheric haze. In the LiDAR data quick-look panels, the range-corrected return signal increases with the increase of backscattering of the atmospheric layers which is usually caused by the accumulation of the atmospheric aerosol particles. From Fig.3, we find that most of LiDAR signals relating to aerosol particles are constrained below 2 km or lower than 500 m during severe haze pollution. The LiDAR observation found also that with the development of haze pollution, atmospheric boundary layer height could be decreased to as low as 400 m (Zhang, et al., 2013) and thus formed a kind of "reflection mirror" effect which suppressed the upward spread of the surface level pollution. Furthermore, it can depress the

height of pollution layer and increases again the surface level $PM_{2.5}$; (3) the most polluted two days (January 6 and 7) show similar temporal progress. The pollution was slight during daytime but increased from 16:00 (08:00 UTC) to early morning of the next day. This can be explained by the temperature inversion layer appeared during the nighttime and the accumulation of traffic pollution brought by the increased anthropogenic activities at dusk; (4) the dispersion of haze is related directly to the increase of wind speed in the morning of 8 January (Fig.2). The daily averaged AOD (440 nm) after dispersion of the haze is about 0.17 close to the level before the formation of the haze event (e.g. on January 5). This AOD value can be treated as the background reference under the circumstance with favorable spread conditions, e.g., wind speed > 4 m/s.

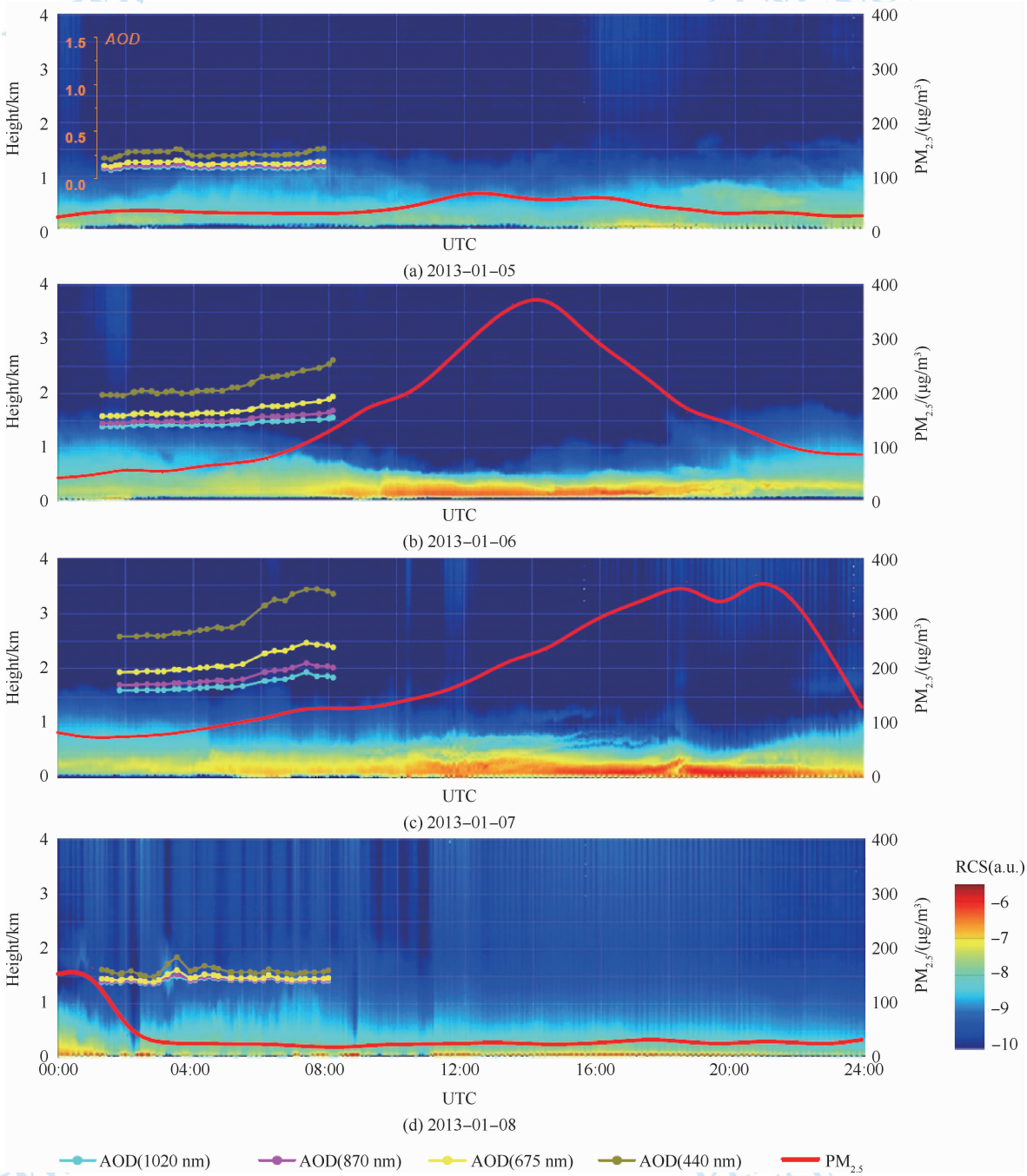

Fig.3 The vertical distribution of haze pollution observed by LiDAR (Range Corrected Signal, RCS) and AOD observed by sun-sky radiometer

From satellite remote sensing, the haze spatial distribution image can be obtained. One can observe directly haze spatial distribution from the satellite raw images thanks to the important influence of haze particles on the atmospheric transmittance. However, the quantitative characterization of haze contents is a challenging task due to difficulties on de-coupling of land-atmosphere effects. Based on red (630—690 nm), green (520—600 nm), blue (430—520 nm) and near infrared (760—900 nm) bands of CCD sensors onboard HJ-1 satellite (Xu, et al., 2013), we can retrieve the high spatial resolution aerosol optical depth by the joint use of multi-wavelength, multi-day satellite observations. In Fig.4, we retrieved aerosol optical depth at 550 nm

(Fig. 4(c)) of Beijing city (Fig. 4(b)) based on HJ-1 image on 6 January (Fig. 4(a)). During the retrieval, we selected 20 km × 20 km regions of Beijing city and resampled the spatial resolution of HJ-1 data from 30 m to 100 m to improve the signal-to-noise ratio. The AOD obtained in this work is estimated to be uncertainty less than about 0.08 by comparing with ground-based sun-sky radiometer measurements (Zhang, et al., 2013). This AOD uncertainty is mainly caused by sensor calibration, aerosol models and interception of look-up table. Moreover, we preformed the spatial interpolation during contouring the AOD graph in order to express the continuous variation of aerosol spatial distribution. From these retrieval results, we find that (1) aerosol in the urban region expresses significant spatial distribution even under stable atmospheric conditions. The high spatial resolution satellite remote sensing results show that the AOD difference of Beijing city in this image reaches about two times (0.48 vs. 0.21). This can be explained by the difference of regional emission sources, e.g. traffic, heating and restaurants (Wen & Hu, 2007). Moreover, the AOD spatial difference can be much larger in the case of invading of outside haze pollution (Zhang, et al., 2013); (2) the retrieved AOD at the validation site is about 0.34 which is very close to that of ground-based sun-sky radiometer (0.33). This proves that satellite observation obtains well the aerosol optical depth; (3) the averaged AOD of the image is about 0.30 which is less than the normal haze level. By comparing with Fig.3, we find that the haze pollution is not yet formed during the satellite passing time (03:30 UTC on 6 January 2013) and AOD and $PM_{2.5}$ are still under the lower levels.

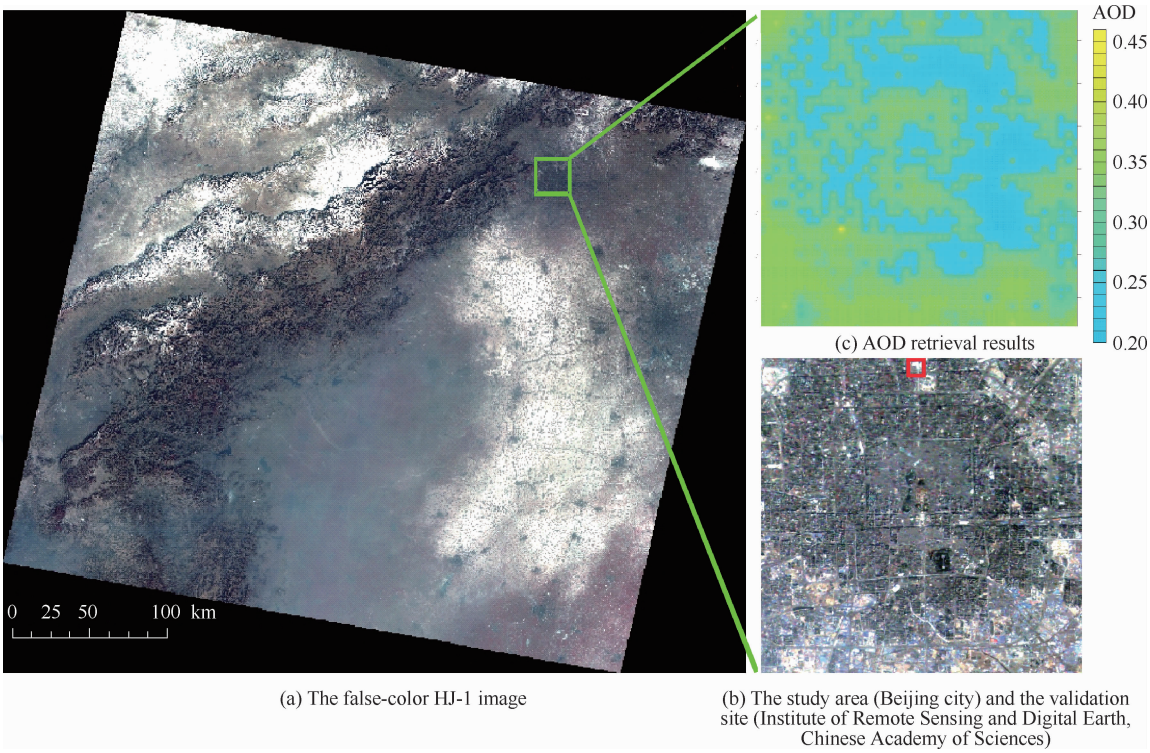

(a) The false-color HJ-1 image

(b) The study area (Beijing city) and the validation site (Institute of Remote Sensing and Digital Earth, Chinese Academy of Sciences)

(c) AOD retrieval results

Fig.4 Haze spatial distribution obtained from CCD sensors of HJ-1 satellite (January 6, 2013)

3 CONCLUSIONS

Remote sensing can provide stereoscopic monitoring of the haze pollution with the advantage of nondestructive observation of ambient atmospheric particles. Focusing on observation of severe haze pollution in January 2013 at Beijing, we conclude that (1) haze aerosols are characterized by complex characteristics and various parameters while the stereoscopic monitoring can provide comprehensive knowledge on their properties. With the example of 2013 first haze pollution (January 5 to 8), we find that the daytime aerosol optical depth at 440 nm varies from 0.12 to 1.19 while most of atmospheric particles concentrates in the space below than 2 km (in the case of severe pollution 500 meters) based on remote sensing observation. Even under the condition of clear or unpolluted atmosphere, the AOD spatial difference can be 200% at different urban regions; (2) the active remote sensing approaches have advantages under heavy pollution conditions or during nighttime while passive remote sensing can obtain abundant information to yield complex aerosol property parameters. Joint use of passive and active remote sensing can provide complementary observation and validation of each others; (3) a preliminary stereoscopic haze monitoring can be realized by combining spot and vertical measurements of ground based remote sensing sites and surface coverage measurement of satellites. However, limitations of the remote sensing monitoring should be also mentioned except for its advantages like vertical observation, spectral information and spatial coverage. For example, haze information obtained by passive remote sensing corresponds mainly to particle properties of the total column atmosphere, instead of directly surface level $PM_{2.5}$ contents. Therefore, we should construct a synthesized stereoscopic monitoring system by the joint use of various active-passive remote sensing approaches and traditional envi-

ronmental monitoring approaches like in situ $PM_{2.5}$ and chemical analyses, which can provide a more comprehensive observation of atmospheric haze process focusing on both spatio-temporal distribution and property characterization aspects, to support the scientific response and control of the haze pollution.

Acknowledgements: We thank Public Meteorological Service Center of China Meteorological Administration for providing visibility, humidity and wind speed data. Authors are also grateful to Beijing Municipal Environmental Monitoring Center and Embassy of the United States at Beijing to provide AQI and $PM_{2.5}$ data.

REFERENCES

Dockery D, Pope C, Xu X, Spengler J, Ware J, Fay M, Ferris B, Speizer F. 1993. An association between air pollution and mortality in six U.S. cities. The New England Journal of Medicine, 329(24): 1753−1759

Pope C, Burnett R, Thun M, Calle E, Krewski D, Ito K, Thurston G. 2002. Lung cancer, cardiopulmonary mortality, and long-term exposure to fine particulate air pollution. The Journal of the American Medical Association, 287(9): 1132−1141

Wen M T and Hu M. 2007. Physical and chemical characteristics of fine particles emitted from cooking emissions and its contribution to particulate organic matter in Beijing. Environmental Science, 28(11): 2620−2625

Xu H, Zhang Y H, Hou W Z, Gu X F and Li Z Q. 2013. Monitoring haze in Beijing based on HJ-1 CCD. Journal of Remote Sensing, 17(2): 476−477

Zhang W C, Zhang Y, Lv Y, Li Z Q, Li K T. 2013. Observation of atmospheric boundary layer height by ground-based LiDAR during haze days. Journal of Remote Sensing, 17(4): 981−992 [DOI:10.11834/jrs.20133075]

Zhang Y H, Li Z Q, Hou W Z, Xu H. 2013. Retrieval of haze aerosol optical depth based on high spatial resolution CCD of HJ-1. Journal of Remote Sensing, 17(4): 959−969 [DOI:10.11834/jrs.20133062]

北京区域2013严重灰霾污染的主被动遥感监测

李正强，许华，张莹，张玉环，陈澄，李东辉，
李莉，侯伟真，吕阳，顾行发

中国科学院遥感与数字地球研究所，国家环境保护卫星遥感重点实验室，北京 100101

摘　要：结合2013年1月北京区域严重灰霾污染，介绍了太阳-天空辐射计、激光雷达、多波段CCD相机等遥感监测手段，分析了地-空基、主-被动等遥感方法获得的灰霾气溶胶特性遥感结果，讨论了不同遥感监测手段的特点及联合使用，结果表明：主动遥感手段在严重污染、夜间等情况下具有观测优势，而被动遥感信息含量大，具有获得气溶胶复杂特性参数的能力；地面遥感点、垂直分布线监测数据与卫星遥感的面观测数据相结合，可以初步实现灰霾的主被动遥感立体监测。

关键词：灰霾，遥感，气溶胶，主被动遥感监测，地基激光雷达

中图分类号：TP751　　**文献标志码**：A

引用格式：李正强，许华，张莹，张玉环，陈澄，李东辉，李莉，侯伟真，吕阳，顾行发. 2013. 北京区域2013严重灰霾污染的主被动遥感监测. 遥感学报，17(4)：919-928

Li Z Q, Xu H, Zhang Y, Zhang Y H, Chen C, Li D H, Li L, Hou W Z, Lv Y and Gu X F. 2013. Joint use of active and passive remote sensing for monitoring of severe haze pollution in Beijing 2013. Journal of Remote Sensing, 17(4): 919-928 [DOI: 10.11834/jrs.20133066]

1　引　言

2013年1月，中国东部自北向南的大部分区域发生了严重的雾霾污染。在北京地区，共发生5次空气质量指数(AQI)超过200(重度污染)的灰霾天气。图1显示了北京市环境保护监测中心在朝阳区奥体中心站的AQI监测结果。从空气质量指数的日变化图上，可清晰看到1月份灰霾的变化过程，大体上可分为1月6日—8日、10日—14日、18日—19日、21日—23日、26日—31日，共5个严重污染过程。上述5个严重污染过程中，北京的首要污染物均为细颗粒物($PM_{2.5}$)。图1还显示了日均$PM_{2.5}$(朝阳区美国驻华大使馆观测)，两者一致的变化趋势说明，$PM_{2.5}$在1月份的严重污染过程中是首要影响因素，是造成严重灰霾天气的主要原因。从$PM_{2.5}$图上可见，该站点5次严重灰霾的极值分别为1月7日、12日、18日、23日、29日。其中，1月12日$PM_{2.5}$日均值达552 μg/m^3，是一类环境空气功能区质量要求(GB3095-2012)浓度限值(75 μg/m^3)的7倍多。1月份$PM_{2.5}$超过环保限定值的天数达23天，占该月的74%，超过或接近重度污染的天数达16天，占该月的52%，这种持续的严重大气污染可对健康造成严重危害(Dockery等，1993；Pope等，2002)，导致心血管、呼吸道等相关疾病患病率上升，并带来其他环境问题。

北京区域2013年1月份严重灰霾污染的形成，与大气持续处于静稳状态密切相关，气象要素的分析有助于了解这次灰霾的变化过程。图2显示了在北京南郊观象台观测的能见度、空气湿度和风速。结合图1可见：(1)能见度与$PM_{2.5}$浓度呈现明显的负相关，说明细颗粒物浓度对大气能见度有显著的直接影响。(2)风速与严重灰霾的消散具有正相关性，随着风速增大，严重灰霾得以消除，能见度显著升高，随着风速减弱，灰霾在大气中得以积聚，能见度持续降低。(3)空气湿度在灰霾极值(如1月12日、23、29日等)形成中起重要作用，高达80%以上的空气湿度为灰霾气溶胶的吸湿增长提供了大量的水汽，导致颗粒物体积的显著增长。

收稿日期：2013-03-26；**修订日期**：2013-05-21；**优先数字出版日期**：2013-05-28

基金项目：国家重大科学研究计划(编号：2010CB950800，2010CB950801)；国家自然科学基金优秀青年科学基金项目(编号：41222007)

第一作者简介：李正强(1977—)，男，研究员，主要从事大气遥感研究。E-mail: lizq@irsa.ac.cn

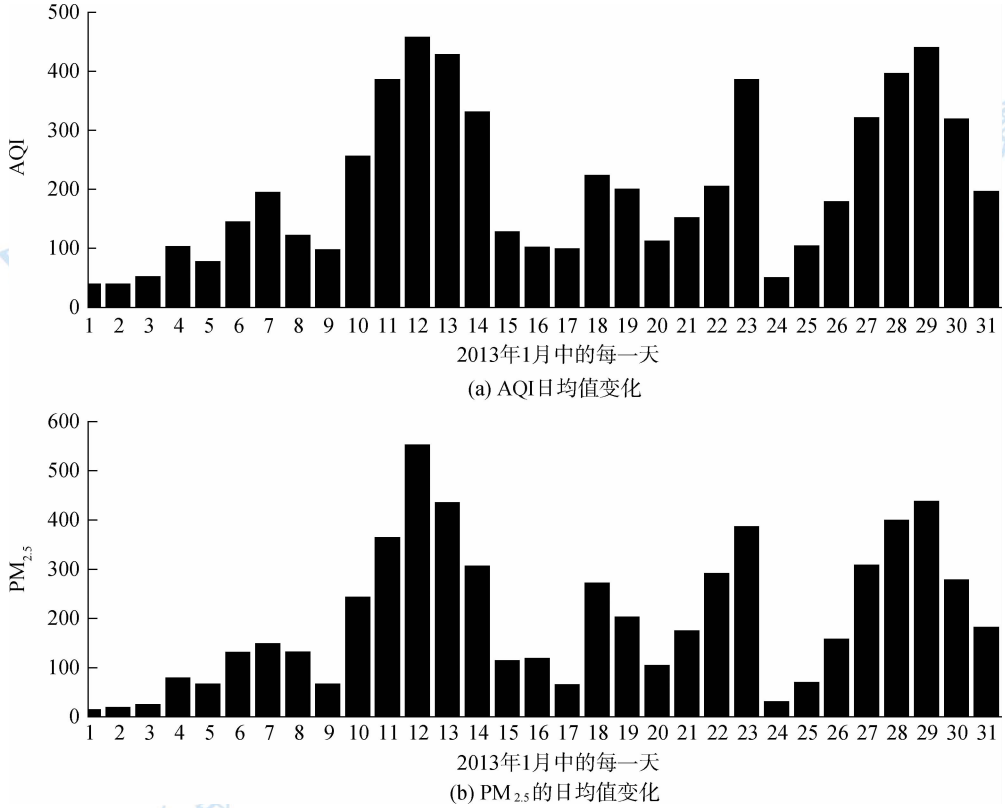

(a) AQI日均值变化

(b) $PM_{2.5}$的日均值变化

图 1　北京市 2013 年 1 月空气质量指数(AQI)和细颗粒物($PM_{2.5}$)含量($\mu g/m^3$)日均值变化

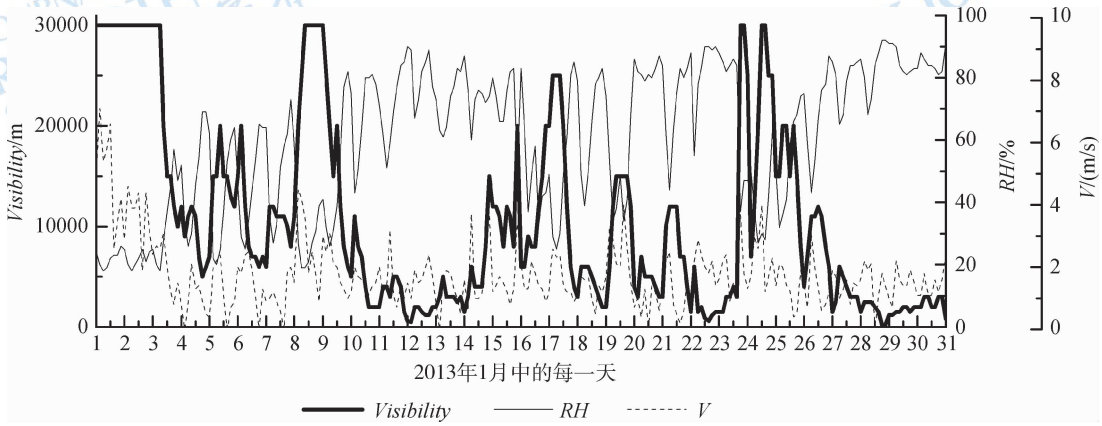

图 2　北京市 2013 年 1 月份能见度(*Visibility*)、空气湿度(*RH*)和风速(*V*)变化图

2　遥感观测分析

结合主被动遥感手段，可以实现对灰霾过程的立体监测。图 3 显示了 2013 年第一次灰霾污染(1 月 5—8 日)的地基激光雷达(采用法国 CIMEL 公司生产的 CE370-2 型，波长 532 nm，激光器类型 Nd:YAG，功率 150 mW)和太阳-天空辐射计(采用法国 CIMEL 公司生产的 CE318-DP 型，波段范围 340—1640 nm)观测结果(站点：中国科学院遥感与数字地球研究所)，图上也同时显示了相距约 10 km 的美国驻华大使馆测量的时平均 $PM_{2.5}$。从图上可以看出：(1)在这次灰霾污染事件中，$PM_{2.5}$ 含量呈现了一个完整的先增高、后降低的过程，太阳-天空辐射计的整层大气气溶胶光学厚度(AOD)观测(440 nm)结果显示最高值为 1.19，是最低值(0.12)的大约 10 倍。同期的近地面 $PM_{2.5}$ 监测结果也显示了基本相同的倍数关系；(2)激光雷达观测结果清晰地显示了大气灰霾的垂直分布和变化情况，距离平方校正回波信号越大，表明该层的后向散射作用越强，这通常是由于气溶胶颗粒物的集聚造成的。从图 3 可见，大部分气溶胶颗粒物信号集中在 2 km 以下，严重灰霾时压低到 500 m 以下。观测研究还发现，灰霾发生

时大气边界层高度可低至 400 m 左右(张婉春 等,2013),形成类似“反射镜”的效应,抑制污染向上扩散,随着污染层压低,$PM_{2.5}$ 显著升高;(3)污染严重的两天(6 日、7 日)均呈现出白天污染较轻,从下午 16 点(08:00 UTC)左右污染开始加重,并持续至第 2 天凌晨的现象。这与夜间逆温层出现相关,也与人类活动带来的晚高峰交通污染堆积有关;(4)灰霾污染的消散与 8 号上午的风速增强(见图 2)直接相关,消散后的 AOD(440 nm)约 0.17(日均值)达到与灰霾污染形成前(5 日)接近的程度,可以认为该值是这一阶段在大气扩散条件良好(例如风速>4 m/s)情况下,北京市区的本底参考值。

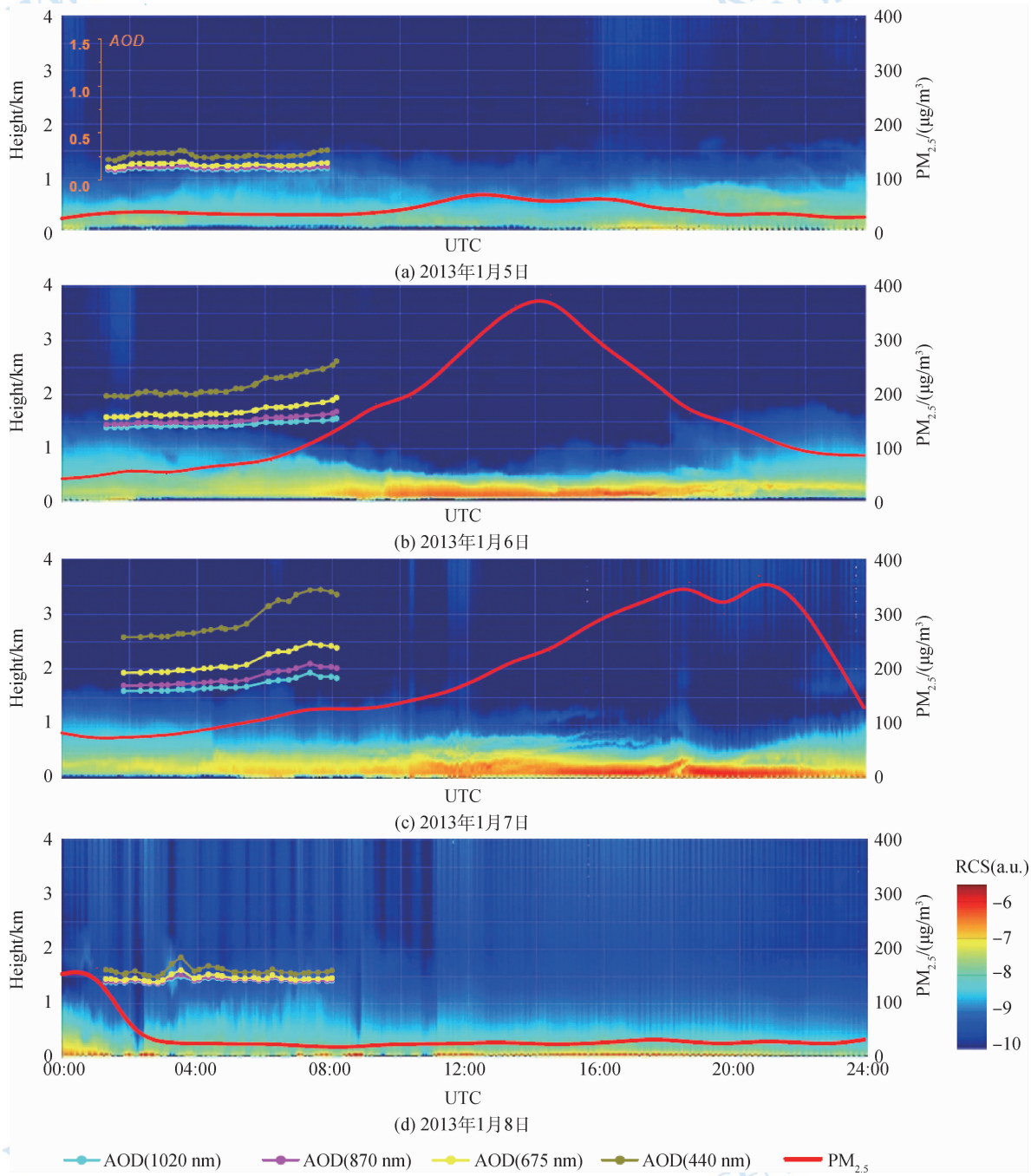

图 3 地基激光雷达灰霾垂直分布监测结果(对数距离平方校正回波信号 RCS)和太阳-天空辐射计观测的气溶胶光学厚度 AOD

基于卫星遥感可获得本次灰霾过程的空间分布图像。由于灰霾污染时,严重影响大气透过率,因此可以从原始图像上较直观的看出其空间区域分布,但定量获取其含量信息却较为困难,需要解

决地气解耦合等问题。中国环境卫星 HJ-1 搭载的 CCD 相机具有红(630—690 nm)、绿(520—600 nm)、蓝(430—520 nm)、近红外(760—900 nm)4 个观测波段(许华等,2013),通过综合使用多波段、多天观测,可以反演城市地区高分辨率的气溶胶光学厚度分布,提供气溶胶空间变化信息。选择 1 月 6 日的 HJ-1 星图像(图 4(a))反演了北京城区(图 4(b))的气溶胶光学厚度(550 nm)分布(图 4(c))。反演时选取了北京城区 20 km×20 km 的区域,将 HJ-1 星原始的 30 m 分辨率重采样为 100 m,以提高反演时的信噪比。该方法得到的气溶胶光学厚度,经与地面太阳-天空辐射计观测对比,初步估计绝对误差小于约 0.08(张玉环 等,2013),主要来自传感器定标、气溶胶模型、查找表截断等。此外,在绘图时还进行了插值处理,以体现 AOD 空间分布的连续变化特征。

从反演结果可以看出:(1)即使在大气稳定的情况下,城市区域的气溶胶也呈现较显著的空间分布差异,高分辨率卫星遥感结果显示,该时刻北京城区不同区域光学厚度差别可达 2 倍左右(0.48 vs. 0.21)。这种差别可认为主要是由于区域人为排放(例如,交通、取暖、餐饮)等局地污染源的差异造成的(温梦婷 等,2007)。而在另一方面,当外部灰霾入侵时,AOD 的区域差别则往往要大的多(张玉环 等,2013);(2)验证点处反演的 AOD 为 0.34,与地面太阳-天空辐射观测结果(0.33)相差很小,表明卫星反演较好地获取了气溶胶光学厚度;(3)遥感图像上平均气溶胶光学厚度为 0.30,尚未达到通常的灰霾标准,结合图 3 可以清楚的看到,1 月 6 日卫星过境时刻(03:30 UTC)灰霾污染尚未形成,AOD 和 $PM_{2.5}$ 尚处在较低的水平。

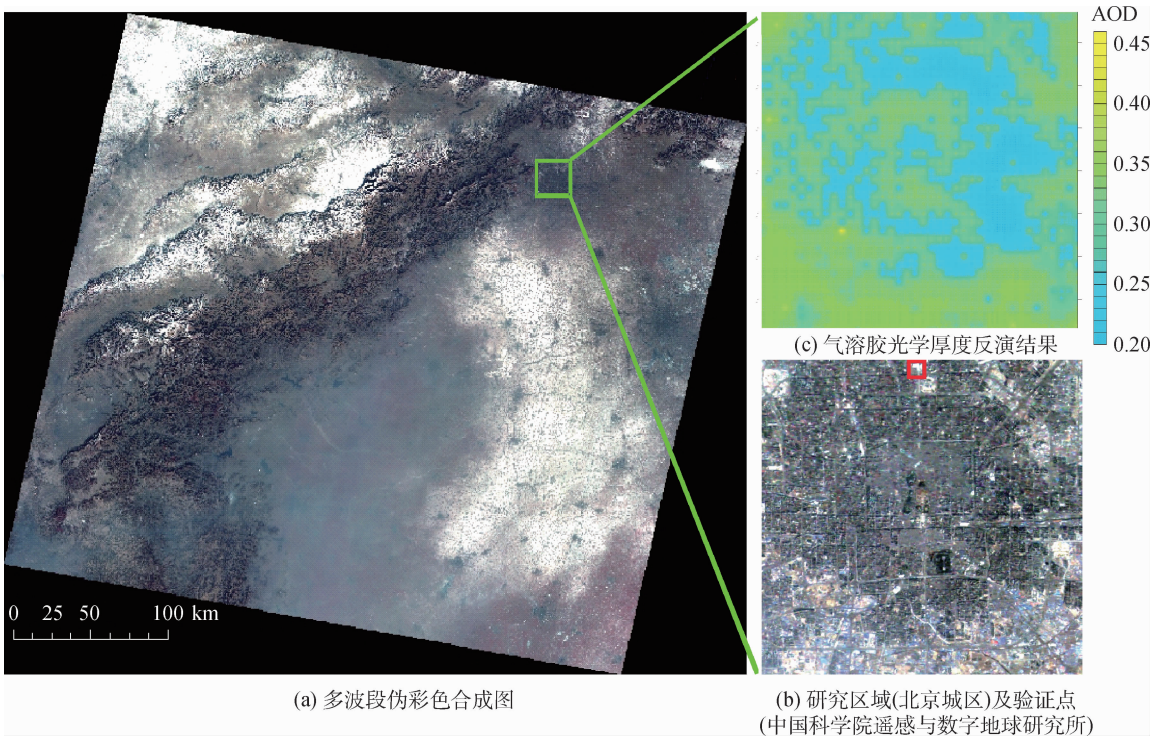

(a) 多波段伪彩色合成图　(b) 研究区域(北京城区)及验证点(中国科学院遥感与数字地球研究所)　(c) 气溶胶光学厚度反演结果

图 4　基于环境星 HJ-1 高分辨率 CCD 传感器的灰霾分布遥感图像(2013 年 1 月 6 日)

3　结　论

遥感监测具有不破坏大气颗粒物存在状态的气溶胶观测优势,能够提供对灰霾污染的立体监测。结合 2013 年 1 月份北京严重灰霾的观测,总结如下:(1)灰霾特性复杂,参数众多,立体监测能够提供对其特性的全面认识。以第一次灰霾(1 月 5 日—8 日)为例,遥感监测获得的昼间气溶胶光学厚度(440 nm)变化范围为 0.12—1.19,大气颗粒物大多积聚在 2 km(严重污染时 500 m)以下高度。即使在晴好天气情况下,城区气溶胶光学厚度的差别也可达 2 倍,具有显著的区域差异;(2)主动遥感手段在严重污染、夜间等情况下具有观测优势,被动遥感信息含量大,具有获得气溶胶复杂特性参数的能力。主被动遥感手段结合可以互补、验证,形成协同观测;(3)地面遥感点和垂直分布线监测数据,与卫星遥感的面观测数据结合,可以初步获得灰霾的立体监测。但同时也应该看到,遥感监测在能够获得灰霾的独特信息(例如垂直分布、光谱信息、空间

分布等)的前提下,也有其局限性,例如往往获得的是整层大气的颗粒物信息,而不是直接的近地面层 $PM_{2.5}$ 含量。因此,应当结合各种主被动遥感手段,以及环保常规监测手段(例如 $PM_{2.5}$ 在线监测、采样分析等),构建一个立体综合监测系统,从时空分布和参数特性两方面,获得大气灰霾过程的更全面观察,为应对和治理大气灰霾提供科技支撑。

志 谢 感谢国家气象局公共气象服务中心提供能见度、空气湿度和风速数据,感谢北京市环境保护监测中心提供 AQI 数据,感谢美国驻华大使馆提供 $PM_{2.5}$ 数据。

参考文献(References)

Dockery D, Pope C, Xu X, Spengler J, Ware J, Fay M, Ferris B, Speizer F. 1993. An association between air pollution and mortality in six U.S. cities. The New England Journal of Medicine, 329(24): 1753-1759

Pope C, Burnett R, Thun M, Calle E, Krewski D, Ito K, Thurston G. 2002. Lung cancer cardiopulmonary mortality, and long-term exposure to fine particulate air pollution. The Journal of the American Medical Association, 287(9): 1132-1141

温梦婷,胡敏. 2007.北京餐饮源排放细粒子理化特征及其对有机颗粒物的贡献.环境科学,28(11): 2620-2625

许华,张玉环,侯伟真,吕阳,李莉,顾行发,李正强. 2013.利用环境一号卫星监测北京地区雾霾.遥感学报,17(2): 476-477

张婉春,张莹,吕阳,李正强,李凯涛. 2013.利用激光雷达探测灰霾天气大气边界高层高度.遥感学报,17(4): 981-992[DOI:10.11834/jrs.20133075]

张玉环,李正强,侯伟真,许华. 2013.利用 HJ1-CCD 高分辨率传感器反演灰霾气溶胶光学厚度.遥感学报,17(4): 959-969[DOI:10.11834/jrs.20133062]

遥感学报

启功先生创刊题名

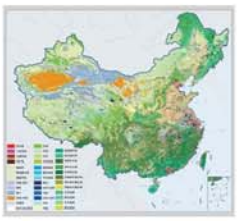

封面说明

About the Cover

2010年中国土地覆被遥感监测数据集（ChinaCover2010）

The China National Land Cover Data for 2010 (ChinaCover2010)

2010年中国土地覆被遥感监测数据集（ChinaCover2010）由中国科学院遥感与数字地球研究所联合其他9个单位历时两年完成，应用30 m空间分辨率的环境星（HJ-1A/1B）数据，利用联合国粮农组织（FAO）的LCCS分类工具，构建了适用于中国生态特征的38类土地覆被分类系统，采用基于超算平台的数据预处理、面向对象的自动分类、地面调查获得的10万个野外样本以及雷达数据辅助分类相结合的方法，数据精度达到85%。ChinaCover2010主要基于国产卫星影像，将遥感与生态紧密结合，充足的野外样点以及严格的产品质量控制在最大程度上保证了数据的精度，可为中国生态环境变化评估以及生态系统碳估算提供基础数据支撑。（网址：http://www.chinacover.org.cn）

The China National Land Cover Data for 2010 (ChinaCover2010) has been completed after two years of team effort by the Institute of Remote Sensing and Digital Earth (RADI), Chinese Academy of Sciences (CAS), together with nine other institutions' participation. The HJ-1A/1B satellite at 30 m resolution is main data source. Based on the landscape features in China, 38 land cover classes have been defined using UN FAO Land Cover Classification System (LCCS). Super computers were used in the data preprocessing. An object-oriented method and a thorough field survey (about 100000 field samples) were used in the land cover classification, with radar imagery as auxiliary data. The overall accuracy of ChinaCover2010 is around 85%. Mainly based on domestic imagery, the products take advantage of various in situ data and strict quality control. ChinaCover2010 is a good dataset for ecological environment change assessment and terrestrial carbon budget studies. (Website: http://www.chinacover.org.cn)

遥感学报

JOURNAL OF REMOTE SENSING

YAOGAN XUEBAO（双月刊　1997年创刊）

第17卷　第4期　2013年7月25日

(Bimonthly, Started in 1997)

Vol.17 No.4 July 25, 2013

主　管	中国科学院	Superintended by	Chinese Academy of Sciences
主　办	中国科学院遥感与数字地球研究所 中国地理学会环境遥感分会	Sponsored by	Institute of Remote Sensing and Digital Earth,CAS The Associate on Environment Remote Sensing of China
主　编	顾行发	Editor-in-Chief	GU Xing-fa
编　辑	《遥感学报》编委会 北京市安外大屯路中国科学院遥感与数字地球研究所 邮编：100101　电话：86-10-64806643 http://www.jors.cn E-mail:jrs@irsa.ac.cn	Edited by	Editorial Board of Journal of Remote Sensing Add: P.O.Box 9718, Beijing 100101, China Tel: 86-10-64806643 http://www.jors.cn E-mail: jrs@irsa.ac.cn
出　版	科学出版社	Published by	Science Press
印刷装订	北京科信印刷有限公司	Printed by	Beijing Kexin Printing Co. Ltd.
总 发 行	科学出版社 北京东黄城根北街16号 邮政编码：100717 电话：86-10-64017032 E-mail:sales_journal@mail.sciencep.com	Distributed by	Science Press Add: 16 Donghuangchenggen North Street, Beijing 100717, China Tel: 86-10-64017032 E-mail: sales_journal@mail.sciencep.com
国外发行	中国国际图书贸易总公司 北京399信箱　邮政编码：100044	Overseas distributed by	China International Book Trading Corporation Add: P.O.Box 399, Beijing 100044, China

中国标准连续出版物号：ISSN 1007-4619 / CN 11-3841/TP

CODEN YXAUAB

国内邮发代号：82-324

国外发行代号：BM 1002

定价：70.00元

ISSN 1007-4619

国内外公开发行